Electrochemistry Communications 34 (2013) 312–315

Contents lists available at ScienceDirect

Electrochemistry Communications

journal homepage: www.elsevier.com/locate/elecom

Short communication

ZnO/graphene nanocomposite fabricated by high energy ball milling with greatly enhanced lithium storage capability

Mingpeng Yu [a,b], Dali Shao [c], Fengyuan Lu [b], Xiang Sun [b], Hongtao Sun [b], Tao Hu [b], Gongkai Wang [b], Shayla Sawyer [c], Hong Qiu [d], Jie Lian [b,*]

[a] Department of Chemistry, Tsinghua University, Beijing 100084, China
[b] Department of Mechanical, Aerospace & Nuclear Engineering, Rensselaer Polytechnic Institute, Troy, NY 12180, USA
[c] Electrical, Computer, and Systems Engineering Department, Rensselaer Polytechnic Institute, Troy, NY 12180, USA
[d] Department of Physics, School of Mathematics and Physics, University of Science and Technology Beijing, Beijing 100083, China

ARTICLE INFO

Article history:
Received 18 June 2013
Received in revised form 2 July 2013
Accepted 7 July 2013
Available online 16 July 2013

Keywords:
ZnO
Graphene
Nanocomposite
High energy ball milling
Anode material

ABSTRACT

The ZnO/graphene nanocomposite was synthesized by high energy ball milling and evaluated as an anode material for lithium-ion batteries. EDX elemental mapping indicated that graphene was dispersed homogeneously in the ZnO matrix. The nanocomposite exhibits an initial reversible capacity of 783 mAh/g and maintained a capacity of 610 mAh/g after 500 cycles at 100 mA/g. Moreover, it shows excellent rate capability and cycling stability even at 10,000 mA/g, which can be attributed to the unique structure and the synergistic effect between the nanosized ZnO and graphene.

© 2013 Elsevier B.V. All rights reserved.

1. Introduction

Lithium-ion batteries (LIBs) are the dominant power source for a wide range of electrical and electronic devices, including consumer electronic devices and the automotive applications, such as the hybrid-electric vehicles and plug-in hybrid-electric vehicles [1–5]. As the most commonly used anode material in LIBs, graphite has approached its usable capacity limit due to constraints by the theoretical specific capacity, i.e. 372 mAh/g. In this regard, ZnO has been investigated as an alternative anode material due to a high theoretical capacity of 978 mAh/g. However, severe capacity fading upon cycling was exhibited even at a low current density, caused by its intrinsic low conductivity and large volume change during the charge–discharge process [6–8]. In this regard, hybridize ZnO with carbonaceous materials, such as graphite [6] and carbon nanotubes [9] has been considered as an effective way to enhance electrochemical performance. In recent years, graphene has been extensively investigated for energy storage due to its unique chemical and physical properties [10,11].

Herein, we synthesized ZnO/graphene nanocomposite through high-energy ball-milling (HEBM) method and it shows enhanced electrochemical performance as an anode material for lithium-ion batteries.

2. Experimental

ZnO nanoparticles were created by a top-down wet-chemistry synthesis process [12] and the detailed preparation procedure for the graphene can be found in our previous report [13]. With a powder-to-ball mass ratio of 80:1, 1.2 g of ZnO powders and 150 mg graphene, ZrO_2 grinding balls ($\Phi = 2$ mm) were introduced into a vial (45 mL in volume) mounted on a high-energy planetary micro mill pulverisette 7 (Fritsch GmbH. Inc., Germany). The ball-milling treatments were performed with a rotatory speed of 500 rpm at room temperature under air atmosphere for 20 h. To avoid the increase in temperature during milling process, the milling treatment was interrupted every 2 h and rested for 1 h.

The morphologies and microstructures of the products were characterized by field emission scanning electron microscopy (FESEM, Zeiss 1540 EsB), X-ray diffraction (XRD; PANanalytical) with Cu Kα radiation ($\lambda = 1.54$ Å) and transmission electron microscopy (TEM, JEOL 2011) operated at 200 keV.

CR2025 coin cells were fabricated in a glove box (MBraun, LabStar) for electrochemical measurements. The nanocomposite was mixed with carbon black (Super-P) and a polyvinyl difluoride (PVDF) binder at the weight ratio of 75:10:15 in methyl-2-pyrrolidinone (NMP) solvent. The resultant slurry was then pasted on copper foil and dried at 120 °C for 12 h under vacuum. Lithium foil was used as both counter and reference electrodes and the electrolyte was 1 M LiPF6 in ethylene carbonate (EC)/dimethyl carbonate (DMC) (1:1 in volume). A Celgard

* Corresponding author. Tel.: +1 5182766081; fax: +1 5182766025.
E-mail address: LIANJ@rpi.edu (J. Lian).

1388-2481/$ – see front matter © 2013 Elsevier B.V. All rights reserved.
http://dx.doi.org/10.1016/j.elecom.2013.07.013

2340 membrane was used as the separator. Galvanostatic charge/discharge cycles were tested using an ARBIN BT 2010 battery analyzer between 2.5 and 0.01 V versus Li/Li^+ at room temperature. Cyclic voltammogram (CV; 0.01–2.5 V, 0.5 mV s^{-1}) tests were conducted on an electrochemical workstation (Ametek, Princeton Applied Research, Versa STAT 4).

3. Results and discussion

FESEM images of the pristine ZnO and ZnO/graphene nanocomposite are shown in Fig. 1a and b, respectively. The sizes of the pristine ZnO range from tens of nm to 150 nm. Fig. 1b shows the nanocomposite mainly composed of two components: (i) spindle-like ZnO with an average width of about 25–35 nm and a length up to 100 nm, which are the fragments of large ZnO nanoparticles, and (ii) tiny ZnO nanoparticles with size less than 20 nm are widely distributed among the nanocomposite. Agglomeration could be caused by the increased surface energy when the particle size is decreasing.

The XRD patterns of pristine ZnO and nanocomposite are presented in Fig. 1c. All the diffraction peaks can be well-indexed to hexagonal ZnO (JCPDS No. 86-1451) without any impurities, indicating that no chemical reaction had taken place during the ball milling process. Furthermore, broadening of the diffraction peaks is observed, confirming that the average ZnO particle size is significantly reduced. The average ZnO crystallite sizes are 80 and 15 nm before and after ball milling, respectively, as determined using the Scherrer formula. The elemental mapping images (Fig. 1d–f) clearly reveal that the ZnO was homogeneously dispersed in the graphene matrix.

The nanocomposite was further analyzed by TEM and high resolution (HR) TEM. Large amounts of graphene confined ZnO nanocrystallites (~2–5 nm) could be observed in Fig. 2a. The original graphene was crushed into much smaller pieces, which agglomerated with nanosized ZnO to reduce the high surface energy. In Fig. 2a, the stack of graphene is clearly visible (cf. black arrows). In the ball milling process, lots of dangling bonds and open edges could be generated with high chemical reaction activity [14], establishing the nanocomposite as a good candidate in energy storage or for electrochemical applications. Fig. 2b shows a HRTEM image of the nanocomposite, from which the (002) lattices of ZnO nanocrystallite can be clearly identified from the interplanar distance of 0.26 nm. HRTEM (Fig. 2c) shows that the tip of the spindle-like ZnO forms lamellar microstructure. High density of dislocations caused by applied stress could be observed (Fig. 2d), which can be the result of HEBM by ZrO_2 balls.

The electrochemical performance of the nanocomposite is shown in Fig. 3. The first five charge–discharge curves of the nanocomposite electrode are shown in Fig. 3a. The first discharge capacity is 1350 mAh/g,

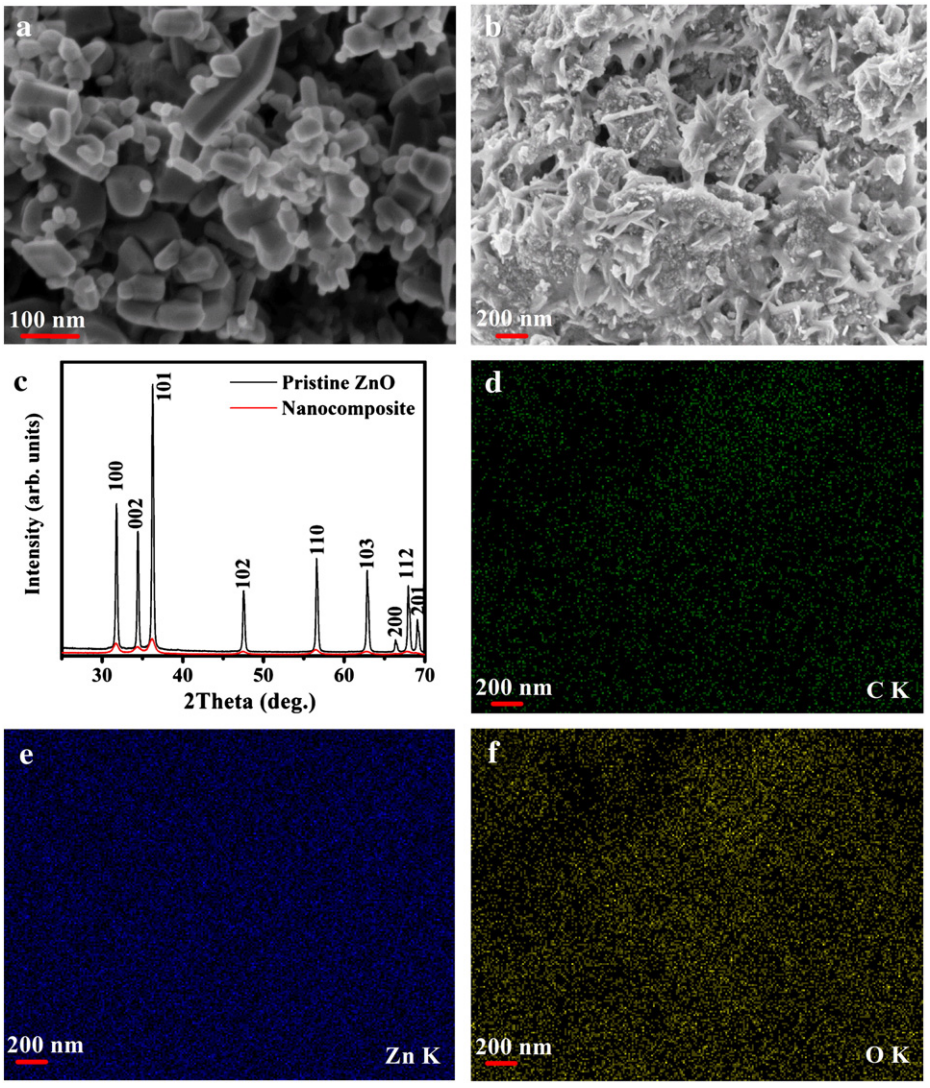

Fig. 1. SEM images of (a) pristine ZnO, and (b) ZnO/graphene nanocomposite. (c) XRD patterns of pristine ZnO and nanocomposite. EDX elemental mapping of (d) C, (e) Zn and (f) O of the nanocomposite.

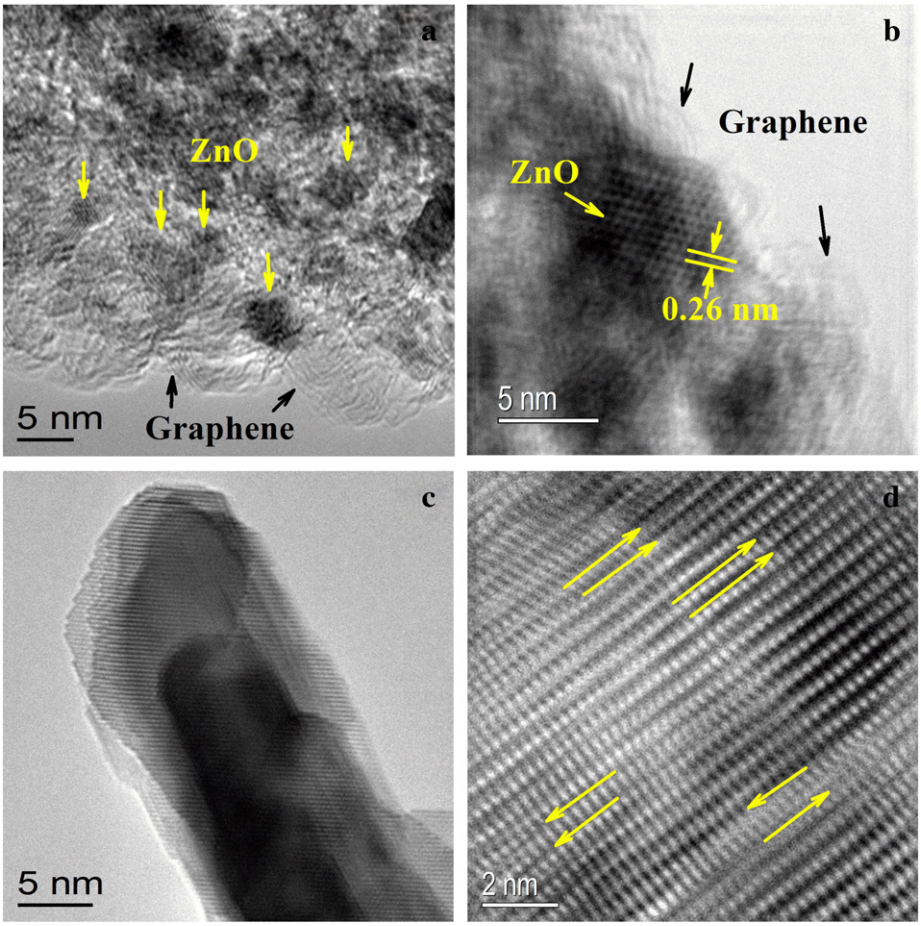

Fig. 2. (a) Low magnification TEM image of ZnO/graphene nanocomposite. (b) HRTEM image of ZnO/graphene nanocomposite. (c, d) HRTEM images of ZnO. The arrows in (d) indicate the dislocations.

much higher than the theoretical value of 978 mAh/g. The excess capacity could originate from electrolyte decomposition in the low-potential region, formation of solid electrolyte interface (SEI) layer and perhaps abundant surface defects as well as the good dispersity of the ZnO nanocrystallites, which would enhance the surface electrochemical reactivity and improve Li ion storage capacity [15,16].

Fig. 3b shows the CV curves of the nanocomposite electrode. In the first cycle, two cathodic peaks are observed at about 0.50 and 0.05 V. The strong reduction peak at 0.05 V is due to the insertion of Li into graphene, suggesting that the graphene is electroactive for lithium storage. The broad peak at about 0.5 V in the first cathodic curve is related to a combination of several electrochemical reactions with close potentials, such as the reduction of ZnO to Zn, the alloying reaction between Li and Zn, and the formation of the solid electrolyte interface (SEI) layer [7,17]. The peaks located at about 0.7 and 1.4 V can be ascribed to the multi-step de-alloying process of Li–Zn alloy. In the second cycle, the cathodic peak shifts from 0.5 V to a higher potential of 0.74 V while the anodic peaks coincide with those in the first scan. After the third scan, the reduction and oxidation peaks, associated with the Li-alloying/de-alloying processes, almost coincide with each other, suggesting a good electrochemical reversibility.

Fig. 3c shows long-term cycling performance and the corresponding coulombic efficiency of the nanocomposite at 100 mA/g. The nanocomposite delivers an initial reversible capacity of 783 mAh/g and maintains a capacity of 610 mAh/g after 500 cycles. The stable reversible capacity as well as the high coulombic efficiency indicates the integrity of the nanocomposite electrode. More importantly, the nanocomposite electrode exhibits a significantly improved cycling performance than bare ZnO and graphene after ball milling (Fig. 3c), denoting strong synergism [18]. Also, the HEBM method has great advantage over hand-grinding, demonstrating significant improvement in the electrochemical performance. For comparative purposes, electrode prepared with 50 mg graphene exhibits much worse performance (Fig. 3c) than that with 150 mg. With appropriate amount of graphene, the volume change of ZnO upon lithium uptake and removal could be minimized more efficiently by the mechanical buffering of the graphene. In the meantime, the intimate contact of ZnO with graphene ensures that the electrical contact throughout the whole nanocomposite during cycling, electrical continuity and structural integrity can be maintained.

Another electrochemical characteristic associated with nanocomposite is the excellent rate capability. The nanocomposite electrode exhibits excellent rate capability at various rates between 100 and 10,000 mA/g (Fig. 3d). Moreover, after being cycled at high rates, the capacity can be well recovered once the current density is shifted to the original low value, indicating the excellent reversibility of nanocomposite electrode. The superior electrochemical performance of the nanocomposite, with highly reversible capacity, stable cycling behavior and excellent rate capability could be attributed to the buffering, confining, conducting and synergistic effects of the incorporated graphene.

4. Conclusion

In summary, ZnO/graphene nanocomposite was obtained via HEBM method and further used as an advanced anode material for high performance LIBs. The nanocomposite exhibits high specific capacity, excellent cyclability and high rate capability. The excellent electrochemical properties can be attributed to the synergistic effect between the ZnO nanocrystallites and graphene. Our results suggest a new way to improve

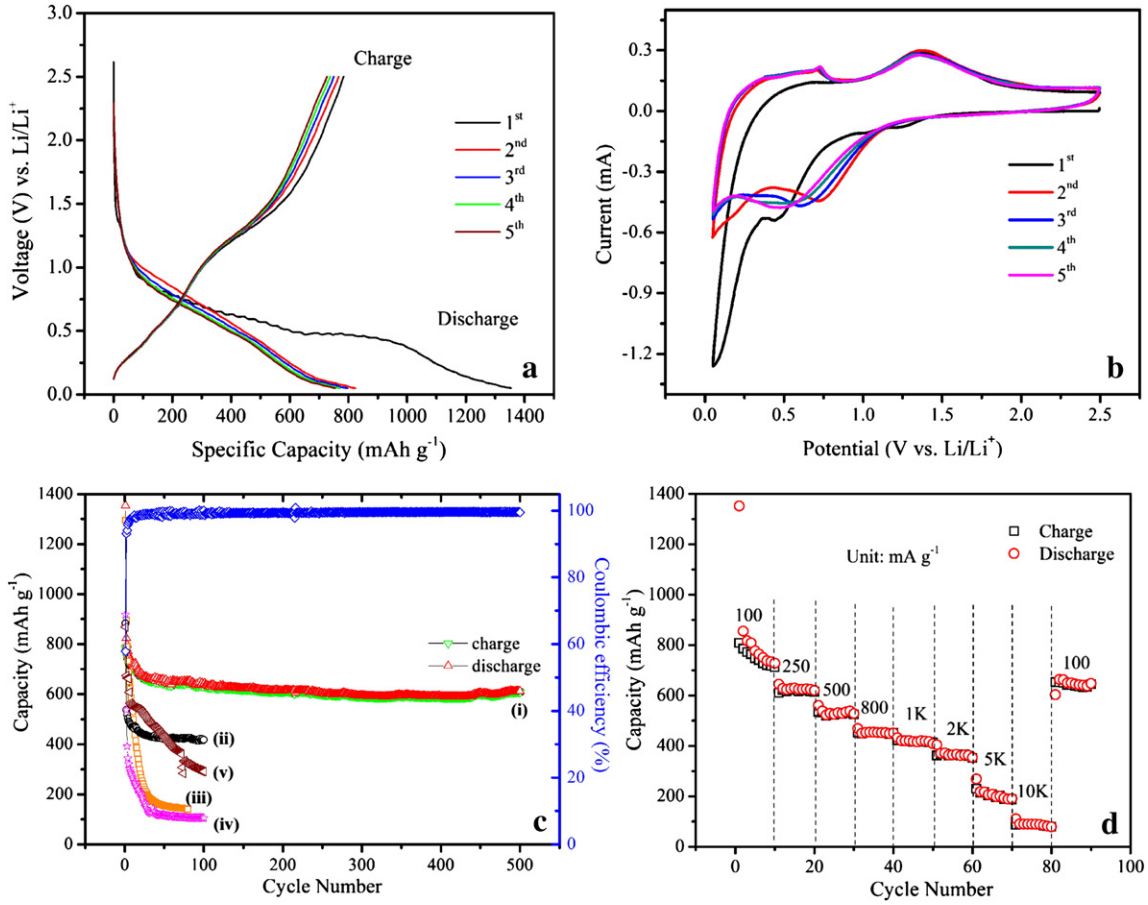

Fig. 3. (a) Charge–discharge curves of ZnO/graphene nanocomposite at 100 mA/g. (b) CV curves of the nanocomposite at 0.5 mV/s. (c) Comparison of the cycling performance of (i) ZnO/graphene nanocomposite, (ii) bare ZnO, (iii) bare graphene, (iv) ZnO/graphene nanocomposite with 50 mg graphene and (v) hand-grinding at 100 mA/g, respectively. (d) Rate capability of the nanocomposite at various current rates.

the electrochemical properties of ZnO-based anode material for high performance LIBs.

Acknowledgments

This work was supported by a NSF career award under the Award number of DMR 1151028. The author Mingpeng Yu thanks the China Scholarship Council (CSC File No. 2010646040) for the financial support.

References

[1] A.S. Arico, P. Bruce, B. Scrosati, J.M. Tarascon, W. Van Schalkwijk, Nature Materials 4 (2005) 366.
[2] M. Armand, J.M. Tarascon, Nature 451 (2008) 652.
[3] J.M. Tarascon, M. Armand, Nature 414 (2001) 359.
[4] X. Ji, K.T. Lee, L.F. Nazar, Nature Materials 8 (2009) 500.
[5] V. Etacheri, R. Marom, R. Elazari, G. Salitra, D. Aurbach, Energy & Environmental Science 4 (2011) 3243.
[6] J. Liu, Y. Li, R. Ding, J. Jiang, Y. Hu, X. Ji, Q. Chi, Z. Zhu, X. Huang, Journal of Physical Chemistry C 113 (2009) 5336.
[7] C. Zhang, J. Tu, Y. Yuan, X. Huang, X. Chen, F. Mao, Journal of the Electrochemical Society 154 (2007) A65.
[8] F. Belliard, J.T.S. Irvine, Journal of Power Sources 97–98 (2001) 219.
[9] M. Baibarac, I. Baltog, T. Velula, I. Pasuk, S. Lefrant, N. Gautier, Journal of Physics: Condensed Matter 21 (2009) 445801.
[10] K.S. Novoselov, A.K. Geim, S.V. Morozov, D. Jiang, Y. Zhang, S.V. Dubonos, I.V. Grigorieva, A.A. Firsov, Science 306 (2004) 666.
[11] K.S. Novoselov, A.K. Geim, S.V. Morozov, D. Jiang, M.I. Katsnelson, I.V. Grigorieva, S.V. Dubonos, A.A. Firsov, Nature 438 (2005) 197.
[12] S. Sawyer, L. Qin, C. Shing, International Journal of High Speed Electronics and Systems 20 (2011) 183.
[13] G. Wang, X. Sun, F. Lu, H. Sun, M. Yu, W. Jiang, C. Liu, J. Lian, Small 8 (2012) 452.
[14] A. Nieto-Marquez, R. Romero, A. Romero, J.L. Valverde, Journal of Materials Chemistry 21 (2011) 1664.
[15] X. Zhu, Y. Zhu, S. Murali, M.D. Stoller, R.S. Ruoff, Journal of Power Sources 196 (2011) 6473.
[16] S. Song-Lin, L. Yong-Gang, Z. Jing-Yuan, W. Tai-Hong, Chinese Physics B 18 (2009) 4564.
[17] J. Liu, Y. Li, X. Huang, G. Li, Z. Li, Advanced Functional Materials 18 (2008) 1448.
[18] Z.-S. Wu, W. Ren, L. Wen, L. Gao, J. Zhao, Z. Chen, G. Zhou, F. Li, H.-M. Cheng, ACS Nano 4 (2010) 3187.